

1 Self-Assembling Elastin-Like Hydrogels for Timolol Delivery: 2 Development of an Ophthalmic Formulation Against Glaucoma

3 Alicia Fernández-Colino,^{†,§,||} Daniela A. Quinteros,^{‡,||} Daniel A. Allemandi,[‡] Alessandra Girotti,[†]
4 Santiago D. Palma,^{*,‡} and F. Javier Arias^{*,†,||}

5 [†]Bioforge Lab, University of Valladolid, CIBER-BBN, Paseo de Belén 19, 47011 Valladolid, Spain

6 [‡]Unidad de Investigación y Desarrollo en Tecnología Farmacéutica (UNITEFA), CONICET and Departamento de Ciencias
7 Farmacéuticas, Facultad de Ciencias Químicas, Universidad Nacional de Córdoba, Ciudad Universitaria, 5000-Córdoba, Córdoba,
8 Argentina

9 **S** Supporting Information

10 **ABSTRACT:** This work focuses on improving the effective-
11 ness of current therapies against glaucoma by incorporating
12 self-assembled polymers into the ophthalmic formulation. To
13 that end, we first studied the influence of the dispersing
14 medium on the mechanical performance of self-assembling
15 elastin-like (EL) and silk-elastin-like (SEL) hydrogels by
16 conducting rheological tests. These polymers were subse-
17 quently incorporated into the antiglaucoma formulation, which
18 contains timolol maleate (TM) as active ingredient, and *in vivo*
19 tests, namely adhesion tests and intraocular pressure measurements (IOP), were performed in New Zealand rabbits. An
20 enhanced reduction in IOP due to the presence of the polymers was observed. Moreover, differences in the effectiveness between
21 both EL- and SEL-hydrogels, which can be explained on the basis of the different rheological properties displayed by these two
22 systems, were also encountered. The results point to the potential of this system as a basis for the development of an ophthalmic
23 formulation against glaucoma.

24 **KEYWORDS:** glaucoma, silk-elastin-like recombinamers, elastin-like recombinamers, thermo-gelling, ophthalmic formulation



1. INTRODUCTION

25 Glaucoma is the second leading cause of blindness worldwide¹
26 and is a multifactorial, progressive and neurodegenerative
27 disease characterized by atrophy of the optic nerve and loss of
28 retinal ganglion cells that can eventually lead to loss of visual
29 acuity and visual field. High intraocular pressure (IOP) is
30 considered to be the greatest risk factor for the development of
31 glaucoma, therefore most treatments involve the chronic
32 application of eye drops containing hypotensive agents.
33 Timolol maleate (TM) is a small, hydrophilic molecule (432
34 Da) which is the US Food and Drug Administration's (FDA)
35 "gold standard" drug for the treatment of high IOP.² Indeed,
36 the IOP-lowering potential of this β -receptor antagonist has
37 been reported to be between 20% and 25% from the initial
38 values.³

39 Topical instillation of this and other hypotensive drugs is
40 preferred in order to minimize systemic side effects.⁴
41 Ophthalmic drug delivery is one of the most interesting and
42 challenging endeavors facing the pharmaceutical sector as the
43 anatomy, physiology, and biochemistry of the eye render this
44 organ exquisitely impervious to foreign substances.⁵ As such,
45 most drugs are hardly absorbed, with bioavailabilities ranging
46 from 1% to 10%. Among other factors, such low bioavailabilities
47 are a consequence of a rapid and extensive loss of the
48 formulation from the precorneal area due to the turnover of

49 lacrimal drainage, which decreases the residence time of the
50 formulation on the eye surface and hampers the efficiency of
51 this route.⁵ Consequently, repeated and frequent applications
52 of topical ophthalmic formulations are usually required to
53 achieve the desired therapeutic effect. Glaucoma treatments are
54 usually associated with adverse reactions generated by frequent
55 exposure of the eye to drugs and excipients. With regard to
56 excipients, preservatives can induce ocular surface alterations
57 that contribute to the development of secondary ophthalmic
58 diseases, such as dry eye syndrome, which, in turn, can
59 compromise patient compliance. However, the elimination of
60 preservatives from ophthalmic formulations is not always
61 sufficient to avoid side effects on the ocular surface. The
62 development of topical ophthalmic formulations for the
63 treatment of this disease therefore presents a challenge.⁶ As
64 such, the incorporation of new components with beneficial
65 properties into ophthalmic formulations that are also able to
66 increase the bioavailability of the drug is of great interest in this
67 field.⁷

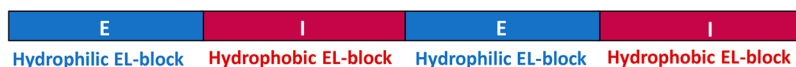
Received: July 17, 2017

Revised: October 9, 2017

Accepted: November 10, 2017

Published: November 10, 2017

a) ELR tetrablock copolymer: (EI)_x2



b) SELR copolymer: (EIS)_x2

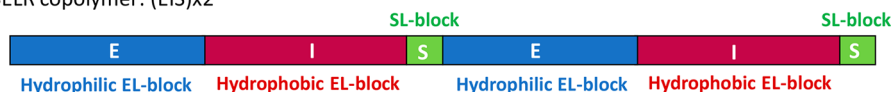


Figure 1. Schematic diagram showing the different domains of the recombinamers (EI)_x2 and (EIS)_x2.

68 The incorporation of viscosifying agents that are able to
69 increase the residence time of the formulation in the eye is
70 gaining increasing attention. Among these compounds, in situ
71 gel-forming formulations, which undergo a phase transition
72 from a liquid to a semisolid gel upon exposure to physiological
73 environments, are a promising approach. These formulations
74 should be free-flowing liquids at room temperature to allow
75 easily reproducible administration into the eye as a drop. They
76 should also undergo an in situ phase transition to form a gel
77 that is able to withstand shear forces in the cul de sac and of
78 sustaining drug release under physiological conditions.⁸ As
79 such, biomaterials science is fast becoming a cornerstone to
80 help to meet the therapeutic challenges faced by ophthalmol-
81 ogists when treating glaucoma.^{6,9}

82 An excellent approach to *in situ* hydrogel formation takes
83 advantage of the self-assembling nature displayed by some
84 protein-based polymers.¹⁰ Many self-assembling motifs have
85 been explored^{11,12} in materials science, with those inspired by
86 the sequence of elastin¹³ (elastin-like polymers, ELPs), silk¹⁴
87 (silk-like polymers, SLPs) or by a combination of the two (silk
88 elastin like polymers, SELPs) being especially relevant.
89 Furthermore, in order to ensure strict control over the
90 sequence, chain complexity and monodispersity, recombinant
91 DNA technology has been implemented to bioproduce this
92 class of materials, therefore a new term, namely recombinamer,
93 has been established to refer to the polymers produced using
94 recombinant technology.^{15,16}

95 The ELP or their recombinant counterparts, known as
96 elastin-like recombinamers (ELR),¹⁷ are artificial polypeptides
97 that are bioinspired in the natural elastin. The native elastin is
98 an insoluble protein formed by the interaction of various
99 molecules of tropoelastin (its soluble precursor). Tropoelastin
100 is composed of two different types of domains, namely cross-
101 linking domains and elastomeric structural domains, which are
102 formed by repeating sequences as poly(VPG), poly(VPGG),
103 poly(GVGVP), poly(IPGVG), poly(VAPGVG), where V
104 stands for valine, P for proline, G for glycine, A for alanine,
105 and I for isoleucine. The sequences of the elastin-based artificial
106 polymers mimic these patterns, and the vast majority have the
107 formula (VPGXG)_n, where *n* is the number of repetitions and
108 “X” represents any amino acid except proline. An amphiphilic
109 ELR tetrablock copolymer from this family, which contains two
110 different kinds of blocks, and was developed to generate
111 micropatterned biocompatible hydrogels, has been reported
112 previously.¹⁸ The hydrophobic blocks, which follow the
113 patterned poly(IPGVG), are responsible for physical cross-
114 linking of the hydrogel (by means of hydrophobic contacts)
115 when the system reaches body temperature due to the
116 characteristic inverse temperature transition (ITT)¹⁹ experi-
117 enced by these materials. Briefly, this transition involves the
118 conformational change of the hydrophobic elastin-like domain

from a soluble, random state at low temperature to an
119 aggregated state characterized by a succession of β -turns above
120 a specific temperature^{20,21} known as the transition temperature
121 (T_t). The remaining two blocks of the molecule are
122 characterized by the presence of VPGE pentapeptides,
123 where E stands for glutamic amino acid. The amino acid
124 glutamic displays a carboxylate group which is ionized at neutral
125 pH and therefore it provides a hydrophilic character. Therefore,
126 VPGE-containing blocks are a random, soluble state under
127 physiological conditions (37 °C, neutral pH),²² and exert a
128 water-retention function required for an hydrogel state.
129

Silk-like recombinamers are bioinspired by the sequence of
130 silk.²³ One of the most popular motifs is the hexapeptide
131 GAGAGS (where A and S stand for the amino acids alanine
132 and serine, respectively), which is naturally present in the heavy
133 chain of silk fibroin produced by the worm *Bombyx mori*.²⁴ The
134 interest in this domain is due to its ability to mediate
135 irreversible and stable physical interactions by adopting a β -
136 sheet conformation. In this respect, the combination of both
137 kinds of domains has given rise to the so-called silk-elastin like
138 recombinamers. (EIS)_x2, which belongs to this family, is
139 constituted by a combination of EL blocks and SL blocks, with
140 the former being found in a tetrablock, thermally triggered,
141 amphiphilic molecule, equivalent to that of (EI)_x2 (Figure 1).
142 This material self-organizes from a sol state to a stable fibrous
143 gel state.²² In (EIS)_x2, EL blocks clearly dominate the final
144 structure compared to other SELRs found in the literature. The
145 small proportion of SL blocks to EL blocks used in this
146 construct allows to maintain the self-assembling properties of
147 the EL-blocks.
148

Self-assembly processes of protein-based polymers (e.g., ELR
149 and SELR) have been reported to be influenced by environ-
150 mental conditions, such as pH, temperature, and sonication,²⁵
151 and this feature has been exploited to create devices that are
152 able to sense surrounding stimuli.²⁶ Similarly, this fact opens
153 the door to further tuning the properties of a given material by
154 controlling the external inputs to which it is exposed. With
155 regard to ELR self-assembly, it has been reported that the
156 composition of the dispersing medium plays a pivotal role in
157 determining the nanometer-size features of the resulting
158 micelle-like ELR nanoparticles.^{27,28} However, many of these
159 studies have focused on the change of properties on a
160 nanoscale, and little attention has been paid to the possible
161 effects on macroscale performance.
162

In light of the above, this work focuses on determining the
163 influence of such variables on the physical properties of the
164 hydrogel, as well as the translation of such fundamental studies
165 to the practical aim of developing an ophthalmic antiglaucoma
166 formulation. Thus, four different types of aqueous solutions,
167 namely deionized water, glucose 5%, NaCl 0.9%, and PBS
168 (phosphate buffered saline), were selected according to their
169

170 relevance for their envisaged biomedical application, PBS and
 171 NaCl 0.9% and glucose 5% are highly used solutions in
 172 biomedical research and clinics, and the three of them provide a
 173 osmolarity equivalent to that found in physiological conditions
 174 (270–330 mOsmol/L). Deionized water was included as the
 175 control dispersing medium, characterized by the absence of
 176 solutes. *In situ* gelation behavior in these solutions was studied.
 177 Furthermore, the use of both recombinamers as components
 178 of an ophthalmic formulation against glaucoma was also
 179 evaluated by performing *in vivo* irritation tests, adhesion tests
 180 and IOP measurements in New Zealand rabbits.

2. EXPERIMENTAL SECTION

181 **2.1. Materials.** TM was supplied by Parafarm (Buenos
 182 Aires, Argentina) and sodium chloride by Cicarelli Reagents
 183 (Rosario, Argentina). Glucose 5% was supplied by Roux Ocea
 184 (Buenos Aires, Argentina), and (EI)x2 and (EIS)x2 were
 185 produced by recombinant technology and purified by Bioforge
 186 laboratory as reported elsewhere.^{15,18,22} The nomenclature used
 187 for referring to each block contained in each recombinamer is
 188 provided in Table 1 and the amino acid sequences of the
 189 different recombinamers are shown in Table 2.

Table 1. Correspondence of the Abbreviations Used To Name Each Block that Composes Each Recombinamer

block	amino acidic sequence	source of inspiration
E	[(VPGVG) ₂ -(VPGE) ₂ -(VPGVG) ₂] ₁₀	elastin
I	[VGIPG] ₆₀	elastin
S	[(GAGAGS) ₅ G] ₂	silk

190 Deionized water was used in all experiments. PBS
 191 (phosphate buffered saline: KH₂PO₄ 0.0144% (w/v); NaCl
 192 0.9% (w/v); and Na₂HPO₄ 0.0795% (w/v), pH 7.4) and NaCl
 193 were of analytical grade and were used without further
 194 purification.

195 **2.2. Production of (EI)x2 and (EIS)x2.** The gene
 196 sequences encoding for (EI)x2 and (EIS)x2 were available in
 197 the laboratory from previous studies^{18,22} and had been
 198 constructed through standard molecular biologic techniques.
 199 Specifically, we used the iterative- recursive directional ligation
 200 (RDL) method,²⁹ which allows controlled and sequential
 201 concatenation of the gene segments, resulting in a multiblock-
 202 coding gene. The multiblock-coding genes sequences encoding
 203 for (EI)x2 and (EIS)x2 were subcloned into a modified version
 204 of pET-25(+) expression vector. Finally, they were transformed
 205 into the *E. coli* strain BL21 Star (DE3) (Invitrogen) for
 206 subsequent expression and production of the recombinamers.
 207 The purification protocol consisted of sequential rounds of
 208 inverse transition cycling (ITC). The purity and molecular
 209 weight of the recombinamers were routinely determined by
 210 sodium dodecyl sulfate polyacrylamide gel electrophoresis
 211 (SDS-PAGE), NMR (nuclear magnetic resonance) analysis
 212 amino acid analysis, and mass spectrometry (MALDI-TOF/
 213 MS).

2.3. Rheology Tests. The mechanical properties of (EI)x2
 214 and (EIS)x2 hydrogels were measured in a controlled stress
 215 rheometer (AR2000ex, TA Instruments) equipped with a
 216 Peltier plate temperature control. Thus, 350 μL of each
 217 recombinamer solution at 15 wt% in the corresponding
 218 dispersing medium (deionized water, glucose 5%, NaCl 0.9%,
 219 and PBS) were placed on the Peltier plate of the rheometer
 220 precooled to 5 °C. A parallel plate geometry with a diameter of
 221 20 mm was used. Temperature ramp experiments were
 222 performed by heating the sample from 5 to 37 °C. The
 223 heating rate was 2.5 °C/min, and the reverse process (cooling)
 224 was performed under the same conditions. A constant strain of
 225 0.5% (within the linear viscoelastic region) and a frequency of
 226 10 Hz were used.

2.4. Differential Scanning Calorimetry (DSC). DSC
 228 experiments were performed using a Mettler Toledo 822e with
 229 liquid-nitrogen-cooler. Both temperature and enthalpy were
 230 calibrated using a standard indium sample. (EI)x2 and (EIS)x2
 231 samples for the DSC measurements were prepared at 15 wt % in
 232 PBS, NaCl 0.9%, deionized water and glucose 5%. A volume of
 233 20 μL of the corresponding sample was placed inside a standard
 234 40 μL aluminum pan and sealed hermetically. The heating
 235 program for DSC measurements included an initial isothermal
 236 step (5 min at 0 °C to stabilize the temperature and the state of
 237 the tetrablock), followed by heating from 0 to 60 °C at 5 °C/
 238 min.

2.5. In Vitro Erosion Testing of the Recombinamers.
 240 (EI)x2 and (EIS)x2 solutions at 15 wt% (1 mL) were prepared
 241 in dextrose 5% and kept at 35 °C to achieve a gel state. Then,
 242 3.5 mL of buffer solution pH 6.8 was added with gentle shaking
 243 at 50 rpm. At fixed times, 250 μL samples were removed and
 244 replaced by fresh buffer. The erosion of the hydrogels was
 245 determined using Biuret reagent (CuSO₄ at 2% + NaOH at
 246 40%). The concentration of (EI)x2 and (EIS)x2 in the released
 247 medium was determined by UV spectrophotometry at a
 248 maximum absorbance wavelength of 540 nm (UV VIS
 249 TERMO Evolution 300). All experiments were performed in
 250 triplicate.

2.6. In Vitro Drug-Release Studies. Solutions of (EI)x2
 252 and (EIS)x2 (15 wt %) containing TM (0.5 w/v.%) (1 mL)
 253 were prepared and subsequently kept at 35 °C for 10 min to
 254 ensure hydrogel formation. Thereafter, 3.5 mL of buffer
 255 solution pH 6.8 was added with gentle shaking at 50 rpm. At
 256 appropriate intervals, 250 μL samples were removed and
 257 replaced with fresh buffer. The quantity of TM in the release
 258 medium was determined by high-performance liquid chroma-
 259 tography (HPLC, see Section 2.6). Each sample was assayed in
 260 triplicate (*n* = 3). Mathematical analysis was performed by
 261 adjusting the experimental values to the Korsmeyer–Peppas
 262 model.

$$\frac{M_t}{M_\infty} = k \cdot t^n$$

In the above, M_t is the cumulative amount of drug released at
 264 time t , M_∞ is the cumulative amount of drug released at infinite
 265 time, k is a rate constant incorporating characteristics of the
 266

Table 2. Amino Acid Sequence of Each Recombinamer

abbreviated name	amino acid sequence
(EI)x2	MESLLP-{{(VPGVG)2-(VPGE)2-(VPGVG)2}10[VGIPG]60}2-V
(EIS)x2	MESLLP-{{(VPGVG)2-(VPGE)2-(VPGVG)2}10[VGIPG]60}-[V(GAGAGS)5G]2}2-V

267 macromolecular network of the system and the drug, and n is
 268 the release exponent, which is related to the mechanism of drug
 269 release. If $n = 0.5$, the release is governed by Fickian diffusion,
 270 whereas $n = 1$ indicates that molecules are released by surface
 271 erosion; both mechanisms play a role in release for n values
 272 between 0.5 and 1.³⁰

273 **2.7. HPLC Determinations of TM.** The HPLC system
 274 consisted of a Waters HPLC pump and a Waters HPLC
 275 detector set at 295 nm. Samples were chromatographed on a
 276 reversed-phase Luna C18 column (250 × 4.6 mm, 5 mm,
 277 Phenomenex) and a 2 × 8 mm precolumn of the same material,
 278 with the mobile phase having a flow rate of 1 mL/min and
 279 consisting of trifluoroacetic acid 0.05% (v/v) in acetonitrile
 280 (40:60, v/v), which was filtered and degassed before use. The
 281 column was thermostated at 25 °C.

282 **2.8. Cytocompatibility.** The HFF-1 (human foreskin
 283 fibroblast) cell line was used as cell model to test the
 284 cytocompatibility of the recombinamers. Thus, 7500 HFF-1
 285 cells were seeded onto 96-well culture plates, then the culture
 286 medium was removed after 5 h and replaced with 100 μL of the
 287 corresponding recombinamer solution at 25 μM in culture
 288 medium (DMEN). A 100 μL aliquot of DMEN (with no
 289 recombinamer) was added in the case of the negative controls.
 290 Live and dead staining (LIVE/DEAD Viability/Cytotoxicity
 291 Assay Kit, Invitrogen) was used according to the manufacturer's
 292 instructions, and fluorescence intensity emission was measured
 293 at 425 and 620 nm after excitation at 485 and 525 nm
 294 (SpectraMax M5e microplate reader, Molecular Devices),
 295 respectively, after culture for 24 h. The number of live and
 296 dead HFF-1 cells was calculated from the fluorescence intensity
 297 using a calibration curve obtained with known numbers of
 298 HFF-1 cells seeded on 96-well plates (from 1000 to 20 000 cells
 299 per mL, using 100 μL of DMEN medium). Statistical analysis
 300 was performed by one way analysis of variance (ANOVA).
 301 Images of the cells after Live and dead staining were taken with
 302 a Nikon Eclipse Ti-SR (Japan) fluorescence microscope. Three
 303 independent experiments, each in triplicate, were performed for
 304 each recombinamer.

305 **2.9. In Vivo Mucoadhesion Tests.** Solutions of each
 306 recombinamer at 15 wt % with sodium fluorescein at 0.25% in
 307 dextrose solution at 5% were prepared, and 50 μL of the
 308 corresponding solution was placed in the inferior conjunctival
 309 fornix of the right eyes of three rabbits. The left eyes were used
 310 as controls and were treated with 50 μL of commercial
 311 fluorescein at 0.25%.

312 The behavior of each solution in terms of residence and
 313 adherence on the eye surface was evaluated using a binocular
 314 indirect ophthalmoscope (Neitz IO- small pupils, Tokyo,
 315 Japan) and 20 diopter lens (Nikon, Tokyo, Japan) and a score
 316 was calculated for each time point according to the parameters
 317 presented in Table 3. A one-way ANOVA statistical analysis
 318 was performed and the Holm–Sidak method was applied.

319 **2.10. In Vivo Study of the Hypotensive Efficacy: IOP
 320 Determinations.** Experiments were performed in both eyes of
 321 nonsedated normotensive male New Zealand white rabbits (2–
 322 2.5 kg). The animals were kept in individual cages with free
 323 access to food and water and maintained in a controlled 12/12
 324 h light/dark cycle. Animal management procedures conformed
 325 to the ARVO (Association for Research in Vision and
 326 Ophthalmology) resolution on the use of animals in research,
 327 the European Communities Council Directive (86/609/EEC),
 328 and the Institutional Care and Use Committee of the

Table 3. Proposed Score Rating for Evaluating Bioadhesion Intensity *in Vivo*^a

tissue/region	appearance	score
cornea	complete	4
	3/4 cornea	3
	1/2 cornea	2
	1/4 cornea	1
	nothing	0
conjunctival sac	abundant	3
	medium	2
	Scarce	1
	nothing	0
lachrymal meniscus	2 mm	3
	1 mm	2
	thin line	1
	nothing	0
eyelid	wet	0
	not wet	1
nose	wet	0
	not wet	1

^aThe presence of the formulation is assessed by inspecting several regions and tissues in the eye, and a score is assigned according to the observed appearance. A total score encompassing the global behavior of the formulation is obtained by summing the scores obtained for each region.

Chemistry Faculty of Córdoba University (Córdoba, Argentina) reviewed and approved the protocols.

The corresponding recombinamer, namely (EI)x2 or (EIS)-x2, was dissolved at 15 wt % in glucose 5% (w/v) solution with 0.5% TM (Parafarm), then 50 μL of each formulation was placed into the conjunctival fornix of the eye of the rabbits ($n = 15$ for each formulation). As controls for the recombinamer effect, additional rabbits ($n = 20$) were treated with glucose 5% (w/v) solution with TM 0.5% (with no recombinamer). In order to establish the basal IOP of the animals, additional eyes ($n = 18$) were treated with glucose 5% (w/v) solution alone (with no recombinamer or TM). IOP was measured using a Tonovet rebound tonometer (Tiolat, Helsinki, Finland), which allows IOP to be assessed without the need for topical anesthesia. For each eye, IOP was set at 100% with two basal readings taken 30 min before and immediately before the instillation. The evolution of the IOP was measured each hour for a period of up to 8 h.

2.11. In Vivo Ocular Irritation Test. The potential ocular irritancy and/or damaging effects of the samples tested were evaluated using a slightly modified version of the Draize test.³¹ Thus, for each recombinamer sample, a test was carried out on three New Zealand rabbits using a volume of 50 μL of recombinamer solution at 15 wt % in dextrose 5% with TM at 0.5%. This solution was placed in the conjunctival fornix of the right eyes, with the left eyes being used as negative control. The commercial solution Zopiro 0.5% TM (Elea Visual) was used as the negative irritation control. Postexposure evaluations of the conjunctiva, cornea and iris were performed by external observation under adequate illumination, and additional information was obtained using a binocular indirect ophthalmoscope (Neitz IO- small pupils Tokyo, Japan) and 20 diopter lens (Nikon, Tokyo, Japan). For each observation, one drop of fluorescein salt (0.25%) was instilled to contrast the potential corneal injury. The ocular irritation or damage was scored by successive inspections at 0, 30, 60, 90, and 120 min according

to the outcomes listed in Table 4a), and the total score for each formulation at each time point was calculated by summing the

Table 4. Evaluation Parameters for Ocular Irritation^a

(a)		
region	symptoms	score
corneal opacity (most dense area taken for reading)	no opacity or keratitis	0
	opacity or diffuse keratitis, details of iris clearly visible	1
	easy discernible translucent area, details of iris slightly obscured	2
	opalescent regions; no details of iris visible, size of pupil barely discernible	3
	opaque cornea; iris not discernible through the opacity	4
iritis	normal	0
	turbidity in the aqueous humor	2
	deepening of iris rugae and/or iris congestion or swelling, with perikeratic injection	4
	hemorrhage, gross destruction of iris or nonreactivity to light	6
conjunctival redness	normal blood vessel	0
	some blood vessels definitely hyperemic (injected)	1
	diffuse crimson color; individual vessels not easily discernible.	2
	diffuse dark red	3
	chemosis	4
(b)		
total score	formulation effects	
0–1	not irritating	
2–6	mild irritation	
7–11	moderate irritation	
12–14	severe irritation	

^a(a) Scoring proposed for regulatory agencies to evaluate *in vivo* ocular irritation. The total score is calculated from the sum of all scores obtained for the cornea, iris, and conjunctivae. Adapted from refs 31,32. (b) Formulation effects corresponding to each score value.

scores obtained for each region. The effects of the formulation in terms of irritation, namely no irritation or mild, moderate, or severe irritation, were established by comparing the total score obtained for each condition with Table 4b).

3. RESULTS AND DISCUSSION

3.1. Rheology and DSC. Rheological measurements of (EI)x2 and (EIS)x2 at 15 wt % in the four different types of dispersing media under study, namely PBS, NaCl 0.9%, glucose 5%, and deionized water, all of them at physiological pH, were performed in order to check the possible influence of the composition of the different media on the mechanical performance.

Figure 2 shows the recorded \hat{G} (elastic or storage modulus) and \hat{G} (viscous or loss modulus). The gel point is usually considered as the point from which the storage modulus surpasses the loss modulus, which indicates that the sample has transitioned from fluid-like behavior to viscoelastic solid behavior. Therefore, the gelation temperature can be determined as the crossover temperature between \hat{G} - \hat{G} .³³ As shown in Figure 2, at low temperatures, all the samples displayed \hat{G} and \hat{G} values of just a few pascals, and $\hat{G} > \hat{G}$. However, this situation changes for all eight samples (both recombinamers, each in four different types of dispersing

media) in the temperature range 10–22 °C, in which \hat{G} surpasses \hat{G} , indicating gel formation (Table 5), as.³⁴ Additionally, DSC experiments were performed in order to check the T_t of the recombinamers (Figure S1). It is worth noting that the resulting values are close to the temperature gelation values measured by rheology (Table 5). This similarity is due to the gelation mechanism that governs these materials, in which EL moieties undergo conformational changes from an extended state (below the T_t) to a folded one (above the T_t). This folded state involves the establishment of hydrophobic contacts, which result in gel formation. For the four conditions tested, (EIS)x2 displayed a slightly higher gelling temperature (between 1 and 2 °C higher) than (EI)x2 under the same conditions (Table 5). The presence of the hydrophilic amino acid serine in the sequence of the SL motif could be responsible for the observed increase in the gelation temperature for (EIS)x2 with respect to (EI)x2.

As regards (EI)x2, the gel state was not stable over the whole range of temperatures measured when the dispersing media were NaCl 0.9% or PBS (Figure 2a,c). Although a gel state was clearly present at 20 °C, the mechanical performance of the material was markedly decreased at physiological temperature (37 °C). In other words, the gel state was close to disappear for the sample with PBS (Figure 2a) and was almost negligible in the sample with NaCl 0.9% (Figure 2c). It is remarkable that this behavior contrasts with the behavior experienced by the system when the dispersing media were deionized water or glucose 5%, in which there were no signs of instability and the gel states were maintained at 37 °C (the value of \hat{G} was clearly higher than \hat{G} ; Figure 2e,g, and Table 5). This behavior is also patently clear by looking at the tan δ values. Tan δ represents the ratio of viscous modulus (\hat{G}) to elastic modulus (\hat{G}), and it is therefore a quantifier of the dominance of the elastic or the viscous behavior. As shown in Table 3, tan δ values were higher when the dispersing medium was PBS or NaCl than when glucose 5% or deionized water were used, indicating a more viscous and less elastic behavior of the former.

A similar tendency to that observed for (EI)x2 was found for (EIS)x2, namely the presence of NaCl 0.9% and PBS provoked certain instability in the gel state at 37 °C. However, in this case, this instability did not result in the disappearance of the gel state, as \hat{G} was clearly higher than \hat{G} under these conditions (Figure 2). The slight reduction in the mechanical properties of the gel state observed upon warming from 20 to 37 °C when the dispersing medium was NaCl 0.9% or PBS was not encountered when the medium was deionized water or glucose 5%.

In summary, the presence of NaCl 0.9% or PBS exerts a destabilizing effect on the maintenance of the gel state at 37 °C of both (EI)x2 and (EIS)x2 samples. This destabilization is more prominent for (EI)x2 than for (EIS)x2 due to the presence of the SL block in the latter, which is able to improve the mechanical performance.²²

Furthermore, no signs of instability or a reduction in the mechanical performance of (EI)x2 and (EIS)x2 when changing the temperature of the samples from 20 to 37 °C are observed when the dispersing medium is deionized water or glucose 5%. Taken together, these findings point to an influence of the composition of the dispersing medium on the hydrophobic contacts mediated by the EL-blocks. Such blocks are present in both recombinamers and are responsible for triggering the thermo-gelling process of both systems. When the composition of the dispersing media is analyzed, it can be deduced that the

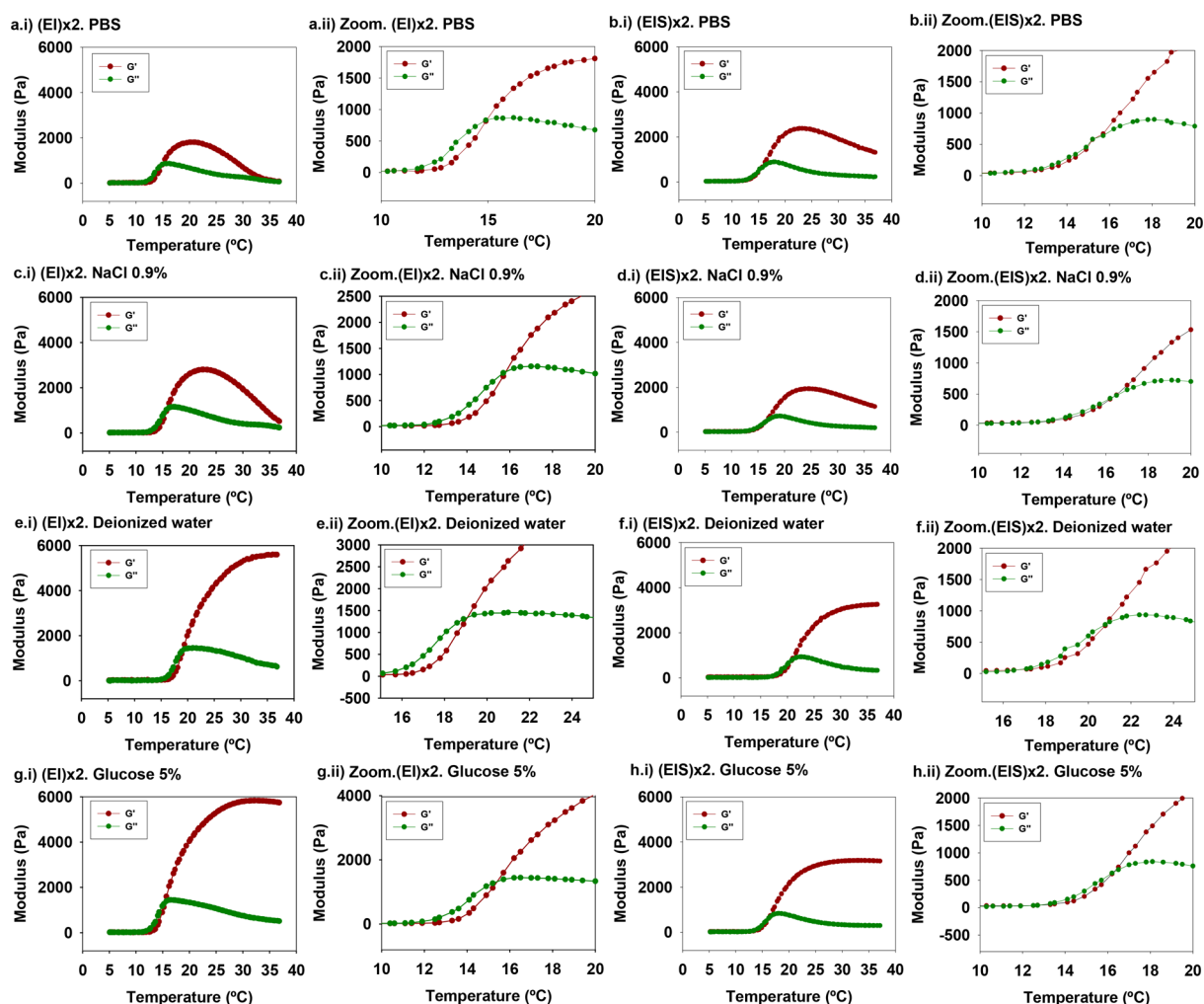


Figure 2. Storage (\hat{G}) and loss moduli (\hat{G}') for (EI)x2 (left) and (EIS)x2 (right) recombinamer solutions (15 wt%) as a function of temperature in different dispersing media. Measurements were performed at 10 Hz. (a) and (b) PBS. (c) and (d) NaCl 0.9%. (e) and (f) Deionized water. (g) and (h) Glucose 5%.

Table 5. (I) Compilation of the Temperatures at which the Crossover between \hat{G} and \hat{G}' Takes Place for (EI)x2 and (EIS)x2 in the Different Dispersing Media, and the Concomitant Complex Modulus (G^*) Obtained at 37 °C for Each Recombinamer and (II) Further Detailed Mechanical Properties (\hat{G} , \hat{G}' , and $\tan \delta$) Displayed by (EI)x2 and (EIS)x2 in Different Dispersing Media at 37 °C

	(I)					
	\hat{G} - \hat{G}' crossover (°C)			G^* (37 °C) (Pa)		
	(EI)x2		(EIS)x2	(EI)x2		(EIS)x2
PBS	18.9	20.8	105	1340		
NaCl 0.9%	15.7	16.5	570	1200		
deionized water	15.7	17.0	5630	3200		
glucose 5%	14.9	15.7	5760	3180		
	(II)					
	(EI)x2			(EIS)x2		
	\hat{G} (Pa)	\hat{G}' (Pa)	$\tan \delta$	\hat{G} (Pa)	\hat{G}' (Pa)	$\tan \delta$
PBS	84	65	0.77	1320	237	0.18
NaCl 0.9%	520	340	0.65	1150	202	0.18
deionized water	5600	623	0.11	3190	331	0.10
glucose 5%	5740	515	0.09	3160	300	0.10

presence of NaCl plays an important role in this destabilization 452 as it is the only component present in both PBS and NaCl 0.9% 453 solutions, and at the same concentration. The destabilization of 454 the gel state exerted by both media is similar, and the $\tan \delta$ 455 values (Table 5, II) clearly point to a decrease in the elastic 456 behavior in both dispersing media (PBS and NaCl 0.9%). 457 However, the remaining components of PBS (i.e., KH_2PO_4 and 458 Na_2HPO_4) seem to accentuate the destabilization of the EL 459 block-mediated gelation to a small extent as the complex 460 modulus (i.e., the overall resistance to deformation, that 461 encompasses both the elastic and the viscous moduli) for 462 (EI)x2 in PBS is slightly lower, and $\tan \delta$ is higher, than in 463 NaCl 0.9% (Table 5). Moreover, the concentration of KH_2PO_4 464 and Na_2HPO_4 in PBS is about 10-times lower than the NaCl 465 concentration, which could explain the almost negligible effect 466 of these compounds on the stability when compared to the 467 marked effect of NaCl. 468

It is also noticeable that the modulus displayed by (EI)x2 in a 469 dispersing medium lacking salts, namely deionized water or 470 glucose 5% (Figure 2e,g), was higher than that displayed by 471 (EIS)x2 (Figure 2f,h). This effect could be explained by the 472 lower amount of EL moieties per molecule in relative terms 473 when comparing (EIS)x2 to (EI)x2. Thus, EL moieties 474 constitute 100% of (EI)x2 molecules but only 90% in the 475

476 case of (EIS)x2. Importantly, neither of these hydrogels was
477 destabilized upon changing the temperature from 20 to 37 °C
478 in these dispersing media.

479 In light of the above, it is clear that dispersing media exert an
480 influence on the mechanical properties of both systems,
481 although the underlying mechanism responsible for the
482 different responses remains unclear. Numerous studies have
483 reported the influence of salts on the ITT behavior of ELRs,
484 and it is well-known that salts cause a concentration-dependent
485 decrease in T_t and an increase in the transition enthalpy.^{27,35}

486 With regard to the nanostructured properties of ELR, NaCl has
487 been reported to have an influence on the size and shape of the
488 resulting nano-objects.²⁷ However, to the best of our
489 knowledge, this is the first time that the influence of salts on
490 the macroscale behavior of an elastin-based material, namely
491 the mechanical performance, has been reported. Diblockcopol-
492 ypeptide amphiphilic polymers containing charged and hydro-
493 phobic segments have been reported to be weakened by the
494 presence of NaCl, and this effect has been attributed to a
495 screening of polyelectrolyte charges, with the authors of this
496 contribution stating that highly charged segments contribute to
497 gel formation.³⁶ Mehta et al. also showed that NaCl can shield
498 electrostatic interactions and impact the modulus of the gels.³⁷

499 In the case in hand, in other words a weakening of the gel state
500 in these elastin-based systems, further research is required in
501 order to understand the underlying molecular phenomena that
502 result in such changes in the rheological properties. However,
503 the aforementioned studies induce us to consider that the
504 interaction between the NaCl and the negative charges of the
505 glutamic residues of the recombinamers (Table 1 and Table 2)
506 may be responsible of the decrease in gel stability.

507 From a practical point of view, glucose 5% was selected as
508 the dispersing medium for (EI)x2 and (EIS)x2 since the
509 stability of both systems (Table 5) is enhanced in this medium.

510 **3.2. In Vitro Drug Release Studies.** Clear difference can
511 readily be seen in the drug-release profiles shown in Figure 3.

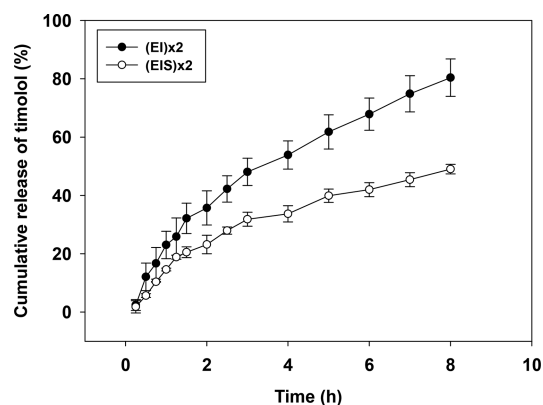


Figure 3. Release profiles of TM from (EI)x2 and (EIS)x2 hydrogels.

512 Specifically, the (EIS)x2 system shows a more sustained release
513 when compared to its (EI)x2 counterpart, with the percentage
514 release after 8 h being 80.39% and 40.04% TM for (EI)x2 and
515 (EIS)x2, respectively. These data point to a relationship
516 between the mechanical properties of the hydrogels and the
517 rate of drug release. Thus, in concordance with its enhanced
518 mechanical performance when compared to (EI)x2, (EIS)x2
519 shows the most sustained release.

520 Drug delivery data were fitted to the Korsmeyer–Peppas
521 model in order to further analyze the experimental results and

to obtain quantitative information that could facilitate the
comparison of both release profiles (Table 6).

Table 6. Values Obtained after Fitting the Drug Delivery Profiles to the Korsmeyer–Peppas, Higuchi, and Zero-Order Kinetics Models

formulations	TM(EI)x2	TM(EIS)x2
	Korsmeyer–Peppas model	
k (hs^{-n})	22.685 ± 0.973	14.930 ± 0.887
n	0.619 ± 0.026	0.588 ± 0.036
R^2	0.988	0.973
	Higuchi model	
k ($\text{hs}^{-1/2}$)	26.988 ± 0.724	16.965 ± 0.469
R^2	0.962	0.958
	zero-order model	
k (hs)	11.831 ± 0.694	7.390 ± 0.496
R^2	0.824	0.764

524 The rate constant k was lower for the (EIS)x2 formulation
525 than for its (EI)x2 counterpart, thus confirming a slower drug
526 release by the former. The n value obtained for (EIS)x2 ($n =$
527 0.58) and for (EI)x2 ($n = 0.62$) points to Fickian diffusion as
528 the main mechanism governing the release. However, erosion
529 processes are also involved in drug delivery as the values
530 obtained are higher than 0.5. Specifically, the n value for (EI)x2
531 is higher than that for (EIS)x2, which points to a higher
532 influence of erosion processes for (EI)x2. Consequently,
533 erosion tests were performed to corroborate this (see next
534 section).

535 **3.3. In Vitro Erosion Testing of the Recombinamers.**
536 Erosion tests were performed in order to determine possible
537 differences in the stability between the two recombinamers. As
538 shown in Figure 4, (EIS)x2 displays a significantly lower

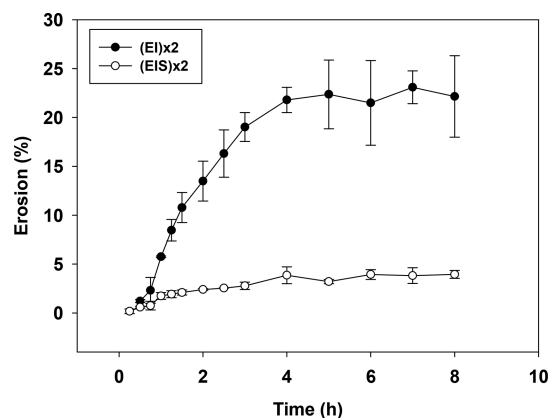


Figure 4. Erosion profiles of (EI)x2 and (EIS)x2 at 15 wt %.

539 erosion than (EI)x2. This is in agreement with the presence of
540 the SL motif in (EIS)x2 as said motif has been reported to
541 provide enhanced stability against erosion in an excess of
542 aqueous media in *in vitro* tests. This performance is likely to be
543 translated into an increase in the residence of ophthalmic
544 formulations containing (EIS)x2. Consequently, the next set of
545 experiments was performed *in vivo* to test this hypothesis.

546 **3.4. Cytocompatibility.** Cytocompatibility assays were
547 performed in order to check the suitability of these
548 recombinamers for biomedical applications. A fibroblast cell
549 line (HFF-1) was used as cell model to test the cytocompat-

550 ability as fibroblasts are the predominant cell type in the ECM
551 and, thereof, represent one of the main portals of exposure to
552 biomaterials. A quantitative analysis was performed by
553 measuring the corresponding fluorescence emitted by both
554 calcein and EtDH-1 under three test conditions, namely HFF-1
555 culture treated with (i) (EI)x2, (ii) (EIS)x2, or (iii) without any
556 recombinamer (control) for 24 h, as detailed in the
557 experimental section.

558 No statistically significant differences in cell viability were
559 found between the treatment groups (Figure 5a) and

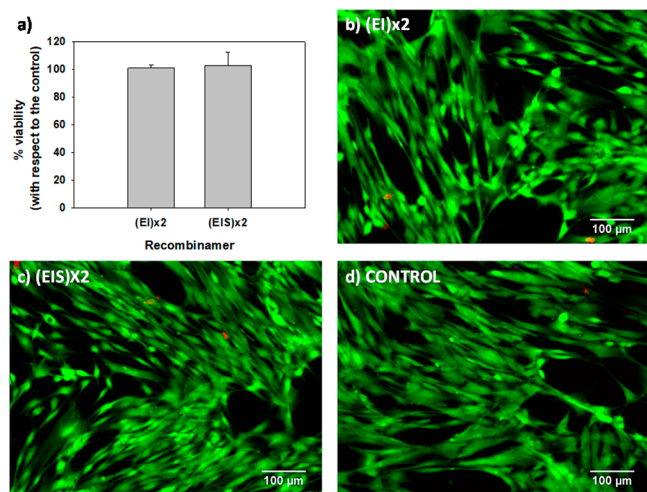


Figure 5. LIVE and DEAD differential staining of HFF-1 cells following 24 h of TC-PS (tissue culture–polystyrene surface) culture in the presence of DMEN medium supplemented with the corresponding recombinamer. (a) Representation of the percentage of viability (with respect to the control) after 24h of culture of HFF-1 cells in the presence of (EI)x2 and (EIS)x2. Three experiments were performed, each in triplicate. Data are expressed as mean \pm standard deviation. (b)–(d) Representative fluorescence microscopy images. Live cells appear in green whereas dead cells appear in red.

560 microscopic observation of the cells corroborated these findings
561 (Figure 5b–d). Furthermore, no morphological differences
562 were observed between the fibroblasts treated with the
563 recombinamers and the control fibroblasts. As such, these
564 results show the cytocompatible nature of these recombinamers
565 and further support their potential application in the biomedical
566 field.

567 **3.5. In Vivo Mucoadhesion Tests.** Adhesion tests were
568 performed in order to determine any differences in retention of
569 the formulation on the eye surface that could potentially affect
570 topical absorption of the drug.

571 Figure 6 shows that, immediately after instillation of the
572 formulations ($t = 0$), adhesion seems to be higher for (EIS)x2
573 than for (EI)x2, with both formulations presenting a higher
574 score than the control, although the apparent differences are
575 not statistically significant. This trend was maintained
576 throughout the study, and between 5 and 15 min, the
577 differences between the three groups were statistically
578 significant, with $p < 0.05$ in all cases. No statistically differences
579 were detected between the control and the formulation
580 containing (EI)x2 between 30 to 45 min, whereas the
581 (EIS)x2 formulation still presented statistically significantly
582 higher adhesion properties, and this formulation could still be
583 detected at 75 min.

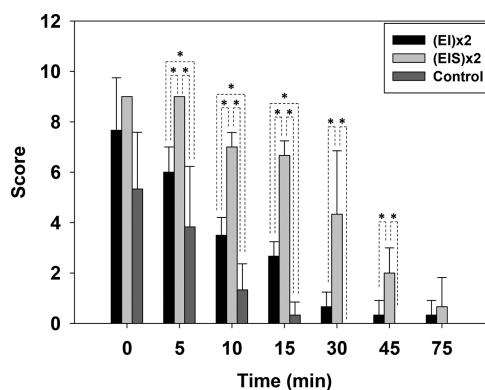


Figure 6. Adhesion score versus time for the recombinamer solutions and control (solution without recombinamer), $n = 3$ rabbits. Data are expressed as mean \pm standard deviation. Statistical significance ($p < 0.05$) is marked with an asterisk.

Thus, formulations containing either of the two recombinamers displayed better adhesion than the control. This is clearly important as regards the development of ophthalmic formulations since rapid washing-out and shear-thinning of mucoadhesive systems is a considerable obstacle that must be overcome when developing drug carriers to be administered in anatomical sites such as the ocular surface, where the clearance time for the tear film is 5–10 s.^{38,39} Herein we show that the incorporation of either of these two recombinamers results in an increase in the residence time of the formulation on the eye surface. Moreover, differences were also detected between (EI)x2 and (EIS)x2, with the latter being more effective at increasing adhesion. This increase in adhesion can be related to the enhanced rheological properties and lower erosion displayed by the (EIS)x2 system when compared to (EI)x2 when NaCl is present, as is the case for the eye surface.

3.6. In Vivo Study of the Hypotensive Efficacy: IOP Determinations. As shown in Figure 7, formulations

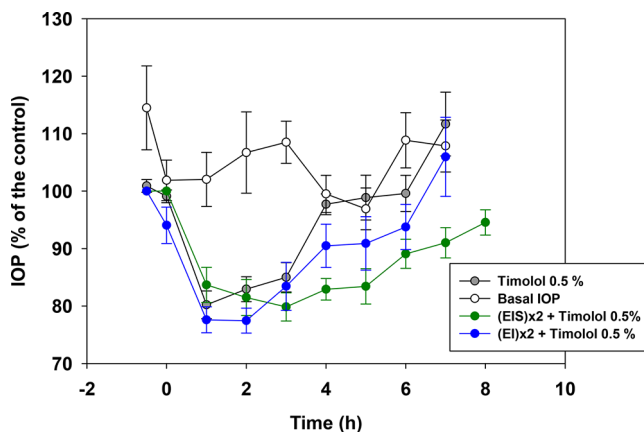


Figure 7. IOP evolution in normotensive New Zealand rabbits after administration of different TM formulations. Gray circles: IOP at different times after administration of TM 0.5% solution in glucose 5% ($n = 20$ eyes). White circles: basal IOP (glucose 5% solution with no hypotensive agent) ($n = 10$ eyes). Green circles: IOP at different times after administration of the formulation containing TM 0.5% in (EIS)x2 at 15 wt % in glucose 5% ($n = 15$ eyes). Blue circles: IOP at different times after administration of the formulation containing TM 0.5% in (EI)x2 at 15 wt % in glucose 5% ($n = 15$ eyes). Data are expressed as mean \pm standard error.

602 containing TM produced a decrease in the IOP, with no
 603 statistical differences being detected between them in the first 3
 604 h. However, this situation changed at 4 h postadministration,
 605 when the IOP for eyes treated with the formulation lacking
 606 recombinamer was statistically significantly higher than that
 607 displayed by the eyes treated with (EIS)x2 ($p < 0.05$). From 4 h
 608 onward, the TM solution presented no hypotensive effects,
 609 while those formulations containing TM and the respective
 610 recombinamer, namely (EI)x2 or (EIS)x2, maintained a
 611 reduced IOP, with this effect being more pronounced for the
 612 formulation containing (EIS)x2. In this case, the hypotensive
 613 effect lasted for more than 8 h.

614 These findings are in concordance with our initial hypothesis,
 615 in which we speculated that elimination of the drug as a result
 616 of lacrimal turnover may be minimized by the use of *in situ* gel-
 617 forming systems, thus leading to an enhanced hypotensive
 618 effect of the formulation. Furthermore, the differences
 619 encountered between (EI)x2- and (EIS)x2-containing systems
 620 agree with an enhanced stability of the latter under saline
 621 conditions. As NaCl constitutes one of the main components of
 622 lacrimal fluid,^{40,41} it is expected to diffuse over time into the
 623 gel-formulation and decrease its mechanical properties,
 624 especially in the case of (EI)x2 (as shown in the rheological
 625 tests). Therefore, it is rational to suppose that the formulation
 626 containing (EIS)x2 displays a longer residence time than its
 627 counterpart containing (EI)x2, as was also demonstrated
 628 experimentally in the *in vitro* erosion tests and the *in vivo*
 629 adhesion tests, thus leading to an increased hypotensive effect.
 630 The results show that the formulation containing (EIS)x2 had a
 631 more sustained effect than a formulation containing just TM, in
 632 which the hypotensive effect lasted only 4 h. Although
 633 hypotensive effects of up to 8 h are also displayed by
 634 commercially available preservative-containing formulations,
 635 such as Timofrol (FrosstLaboratories, Madrid, Spain) or Timolol
 636 Sandoz (Frosst Laboratories),⁴² it is important to note that the
 637 hypotensive effect achieved by the formulation containing
 638 (EIS)x2 was achieved without the use of preservatives. The
 639 inclusion of preservatives, such as benzalkonium chloride,⁴³ is
 640 believed to favor TM penetration, and therefore its therapeutic
 641 efficacy, due to disruption of the hydrophobic barrier of the
 642 corneal epithelium. However, this adjuvant effect is produced at
 643 the expense of an increased toxicity and serious side-effects on
 644 the eye surface.^{44,45} As such, preservative-free antiglaucoma
 645 eyedrops are believed to improve patient compliance and
 646 adherence in the medical treatment of this disease, and the
 647 introduction of preservative-free formulations that maintain
 648 efficacy is an important step toward the development of
 649 ophthalmic solutions.⁴⁶ Moreover, some studies have pointed
 650 to a possible role of the inclusion of polymers in the
 651 antiglaucoma formulations in the reduction of ocular toxicity,
 652 thereby protecting the ocular surface in long-term therapies.⁴²

653 The results reported herein support the feasibility of using
 654 (EIS)x2 as a component in a preservative-free antiglaucoma
 655 formulation while maintaining the efficacy of the commercial
 656 benzalkonium chloride-containing versions. Moreover, the
 657 thermogelling behavior of this system allows easy self-
 658 administration, thus providing an advantage with respect to
 659 other polymeric systems in which preformed scaffolds are
 660 incorporated into the conjunctival sac, which can lead to patient
 661 discomfort.^{47,48}

662 **3.7. In Vivo Ocular Irritation Test.** In order to evaluate the
 663 safety of the formulation containing (EI)x2 or (EIS)x2 15 wt %
 664 with TM at 0.5% in dextrose solution when applied topically to

rabbit eyes, irritation tests were performed as described in the
 experimental section. As shown in Table 7, no irritation was
 666 17

Table 7. Irritation Scores Obtained for the Two Formulations Tested, Namely (EI)x2 and (EIS)x2 Hydrogel at 15 wt % Containing TM 0.5% in the Dispersing Medium Glucose 5% and the Commercial Solution Zopirrol 0.5% TM as Control^a

sample	time (min)			
	30	60	90	120
(EI)x2	0.33 ± 0.58	0.33 ± 0.58	1 ± 0	1 ± 0
(EIS)x2	0.67 ± 0.58	0 ± 0	0 ± 0	0 ± 0
control	0.50 ± 0.55	0.17 ± 0.41	0.33 ± 0.51	0.67 ± 0.51

^aThree rabbits were used for each recombinamer formulation, with the right eyes being treated with the recombinamer solution and the left eyes being treated with the negative control. Data are expressed as mean ± standard deviation. Standard deviation values of zero are possible due to the sensory nature of this class of test.

667 observed for either of the recombinamers as the score was less
 668 than 1 for all the times tested. Moreover, no significant
 669 differences were detected between the recombinamer for-
 670 mulations and the control group. The absence of irritation is in
 671 agreement with the reported biocompatible nature of this class
 672 of materials,⁴⁹ together with the aqueous base of the
 673 formulation and the lack of any preservatives, which maximizes
 674 the potential utility of these devices as drug-delivery systems.

4. CONCLUSIONS

675 Although numerous studies have been conducted in the
 676 development of new antiglaucoma formulations in order to
 677 reduce IOP to a greater extent, further research is still required.
 678 In this sense, the combination of biomaterials science and
 679 pharmacology is a must in order to find new solutions and
 680 approaches to overcome the current problems of ophthalmic
 681 drug delivery. Herein we have evaluated thermosensitive elastin
 682 and silk-elastin-like recombinamers as innovative pharmaceuti-
 683 cal dosage forms for the topical administration of TM.
 684 Aqueous dispersions of recombinamers remained very fluid at
 685 low temperatures, which facilitated drug incorporation and
 686 administration. However, they were able to change into a gel
 687 form at physiological temperature so that TM could come
 688 entrapped inside the gel and experienced a sustained release. *In*
 689 *vivo* studies conducted in New Zealand rabbits showed that the
 690 incorporation of these recombinamers into a pharmaceutical
 691 formulation containing TM prolonged its retention on the
 692 preocular surface, leading to a greater decrease in the IOP. This
 693 effect was more evident in the case of the silk-elastin-like
 694 recombinamer (EIS)x2, which is in agreement with the
 695 enhanced stability of this material in the presence of a saline
 696 aqueous environment, as it is the scenario of the eye surface.
 697 Furthermore, these recombinamers can be placed in the eye
 698 without causing irritating effects or tear turnover, as
 699 demonstrated by the irritation tests, thereby maximizing the
 700 potential utility of these devices as drug-delivery systems.
 701 Therefore, (EIS)x2 constitute a novel and versatile type of
 702 hydrogel to address the critical issues that ophthalmic drug
 703 delivery entails.

In view of the above, and considering the potential offered by
 recombinant technology to develop further designs, the next
 step will focus on the development of a battery of 706
 recombinamers based on these initial designs, in order to 707

708 further improve these outcomes. Specifically, different guest
709 residues will be engineered in the amino acid sequence in order
710 to further increase the retention in the preocular surface,
711 besides facilitating the handling of their aqueous solutions at
712 room temperature.

713 ■ ASSOCIATED CONTENT

714 ● Supporting Information

715 The Supporting Information is available free of charge on the
716 ACS Publications website at DOI: 10.1021/acs.molpharma-
717 ceut.7b00615.

718 DSC scans for 15 wt% (EIS)x2 and (EI)x2 solutions
719 (PDF)

720 ■ AUTHOR INFORMATION

721 Corresponding Authors

722 *E-mail: sdpalma@fcq.unc.edu.ar; Tel. +54-351-5353865.

723 *E-mail: arias@bioforge.uva.es; Tel. +34-983-185855.

724 ORCID

725 F. Javier Arias: 0000-0001-8584-3768

726 Present Address

727 [§]Department of Biohybrid & Medical Textiles (BioTex) at
728 AME-Institute of Applied Medical Engineering, Helmholtz
729 Institute & ITA-Institut für Textiltechnik, RWTH Aachen
730 University, Pauwelsstr. 20, 5207. Aachen, Germany.

731 Author Contributions

732 ^{||}A.F.-C. and D.A.Q. contributed equally to this work.

733 Notes

734 The authors declare no competing financial interest.

735 ■ ACKNOWLEDGMENTS

736 The authors are grateful for the European Social Fund (ESF)
737 and the European Regional Development Fund (ERDF)
738 funding from the EU (NMP-2014-646075, HEALTH-F4-
739 2011-278557, PITN-GA-2012-317306, and MSCA-ITN-2014-
740 642687), the MINECO (MAT2015-68901-R, MAT2016-
741 79435-R, and MAT2016-78903-R), the JCyL (projects
742 VA244U13 and VA313U14), the CIBER-BBN, the Instituto
743 de Salud Carlos III under the “Network Center of Regenerative
744 Medicine and Cellular Therapy of Castilla and Leon”, the
745 assistance of the “Consejo Nacional de Investigaciones Científicas
746 y Técnicas (CONICET)”, and Universidad Nacional de
747 Córdoba.

748 ■ ABBREVIATIONS

749 ELR, elastin-like recombinamer; SELR, silk-elastin like
750 recombinamer; TM, timolol maleate; ITT, inverse temperature
751 transition; ITC, inverse transition cycling; T_t, transition
752 temperature; IOP, intraocular pressure

753 ■ REFERENCES

754 (1) Quigley, H. A.; Broman, A. T. The number of people with
755 glaucoma worldwide in 2010 and 2020. *Br. J. Ophthalmol.* **2006**, *90*
756 (3), 262–267.
757 (2) Marquis, R. E.; Whitson, J. T. Management of glaucoma: focus on
758 pharmacological therapy. *Drugs Aging* **2005**, *22* (1), 1–21.
759 (3) Schmidl, D.; Schmetterer, L.; Garhofer, G.; Popa-Cherecheanu,
760 A. Pharmacotherapy of glaucoma. *J. Ocul. Pharmacol. Ther.* **2015**, *31*
761 (2), 63–77.
762 (4) Nieminen, T.; Lehtimäki, T.; Mäenpää, J.; Ropo, A.; Uusitalo, H.;
763 Kähönen, M. Ophthalmic timolol: Plasma concentration and systemic

cardiopulmonary effects. *Scand. J. Clin. Lab. Invest.* **2007**, *67* (2), 237–
245.
(5) Urtti, A. Challenges and obstacles of ocular pharmacokinetics and
drug delivery. *Adv. Drug Delivery Rev.* **2006**, *58* (11), 1131–5.
(6) Knight, O. J.; Lawrence, S. D. Sustained drug delivery in
glaucoma. *Curr. Opin. Ophthalmol.* **2014**, *25* (2), 112–7.
(7) Quinteros, D.; Vicario-de-la-Torre, M.; Andres-Guerrero, V.;
Palma, S.; Allemandi, D.; Herrero-Vanrell, R.; Molina-Martinez, I. T.
Hybrid formulations of liposomes and bioadhesive polymers improve
the hypotensive effect of the melatonin analogue 5-MCA-NAT in
rabbit eyes. *PLoS One* **2014**, *9* (10), e110344.
(8) Gratieri, T.; Gelfuso, G. M.; Rocha, E. M.; Sarmiento, V. H.; de
Freitas, O.; Lopez, R. F. A poloxamer/chitosan in situ forming gel with
prolonged retention time for ocular delivery. *Eur. J. Pharm. Biopharm.*
2010, *75* (2), 186–93.
(9) Fernandez-Colino, A.; Bermudez, J. M.; Arias, F. J.; Quinteros,
D.; Gonzo, E. Development of a mechanism and an accurate and
simple mathematical model for the description of drug release: Application
to a relevant example of acetazolamide-controlled release from a bio-
inspired elastin-based hydrogel. *Mater. Sci. Eng., C* **2016**, *61*,
286–92.
(10) Altunbas, A.; Pochan, D. Peptide-Based and Polypeptide-Based
Hydrogels for Drug Delivery and Tissue Engineering. In *Peptide-Based
Materials*; Deming, T., Ed.; Springer Berlin Heidelberg: 2012; Vol.
310, pp 135–167.
(11) Zhao, X.; Zhang, S. Molecular designer self-assembling peptides.
Chem. Soc. Rev. **2006**, *35* (11), 1105–10.
(12) Fernandez-Colino, A.; Arias, F. J.; Alonso, M.; Rodriguez-
Cabello, J. C. Amphiphilic Elastin-Like Block Co-Recombinamers
Containing Leucine Zippers: Cooperative Interplay between Both
Domains Results in Injectable and Stable Hydrogels. *Biomacromolecules*
2015, *16* (10), 3389–98.
(13) Rodriguez-Cabello, J. C.; Arias, F. J.; Rodrigo, M. A.; Girotti, A.
Elastin-like polypeptides in drug delivery. *Adv. Drug Delivery Rev.* **2016**,
97, 85–100.
(14) Altman, G. H.; Diaz, F.; Jakuba, C.; Calabro, T.; Horan, R. L.;
Chen, J.; Lu, H.; Richmond, J.; Kaplan, D. L. Silk-based biomaterials.
Biomaterials **2003**, *24* (3), 401–416.
(15) Rodriguez-Cabello, J. C.; Girotti, A.; Ribeiro, A.; Arias, F. J.
Synthesis of genetically engineered protein polymers (recombinamers)
as an example of advanced self-assembled smart materials. In
Nanotechnology in Regenerative Medicine; Navarro, M., Planell, J. A.,
Eds.; Humana Press, 2012; Vol. 811, p 319.
(16) Rodriguez-Cabello, J. C.; Pierna, M.; Fernandez-Colino, A.;
Garcia-Arevalo, C.; Arias, F. J. Recombinamers: combining molecular
complexity with diverse bioactivities for advanced biomedical and
biotechnological applications. *Adv. Biochem. Eng./Biotechnol.* **2010**,
125, 145–79.
(17) Girotti, A.; Fernández-Colino, A.; López, I. M.; Rodríguez-
Cabello, J. C.; Arias, F. J. Elastin-like recombinamers: Biosynthetic
strategies and biotechnological applications. *Biotechnol. J.* **2011**, *6* (10),
1174–1186.
(18) Martin, L.; Javier Arias, F.; Alonso, M.; Garcia-Arevalo, C.;
Rodriguez-Cabello, J. C. Rapid micropatterning by temperature-
triggered reversible gelation of a recombinant smart elastin-like
tetrablock-copolymer. *Soft Matter* **2010**, *6* (6), 1121–1124.
(19) Li, B.; Alonso, D. O. V.; Daggett, V. The molecular basis for the
inverse temperature transition of elastin. *J. Mol. Biol.* **2001**, *305* (3),
581–592.
(20) Urry, D. W. Molecular Machines: How Motion and Other
Functions of Living Organisms Can Result from Reversible Chemical
Changes. *Angew. Chem., Int. Ed. Engl.* **1993**, *32* (6), 819–841.
(21) Tamburro, A. M.; Guantieri, V.; Pandolfo, L.; Scopa, A.
Synthetic fragments and analogues of elastin. II. Conformational
studies. *Biopolymers* **1990**, *29* (4–5), 855–870.
(22) Fernandez-Colino, A.; Arias, F. J.; Alonso, M.; Rodriguez-
Cabello, J. C. Self-organized ECM-mimetic model based on an 830
amphiphilic multiblock silk-elastin-like corecombinamer with a 831

- 832 concomitant dual physical gelation process. *Biomacromolecules* **2014**,
833 *15* (10), 3781–93.
- 834 (23) Numata, K.; Kaplan, D. L. Silk-based delivery systems of
835 bioactive molecules. *Adv. Drug Delivery Rev.* **2010**, *62* (15), 1497–508.
- 836 (24) Hardy, J. G.; Römer, L. M.; Scheibel, T. R. Polymeric materials
837 based on silk proteins. *Polymer* **2008**, *49* (20), 4309–4327.
- 838 (25) Luo, Q.; Dong, Z.; Hou, C.; Liu, J. Protein-based supra-
839 molecular polymers: progress and prospect. *Chem. Commun. (Cam-*
840 *bridge, U. K.)* **2014**, *50* (70), 9997–10007.
- 841 (26) Klaiherd, A.; Nagamani, C.; Thayumanavan, S. Multi-stimuli
842 sensitive amphiphilic block copolymer assemblies. *J. Am. Chem. Soc.*
843 **2009**, *131* (13), 4830–8.
- 844 (27) Pinedo-Martín, G.; Santos, M.; Testera, A. M.; Alonso, M.;
845 Rodríguez-Cabello, J. C. The effect of NaCl on the self-assembly of
846 elastin-like block co-recombinamers: Tuning the size of micelles and
847 vesicles. *Polymer* **2014**, *55* (21), 5314–5321.
- 848 (28) Pinedo-Martín, G.; Castro, E.; Martín, L.; Alonso, M.;
849 Rodríguez-Cabello, J. C. Effect of Surfactants on the Self-Assembly
850 of a Model Elastin-like Block Corecombinamer: From Micelles to an
851 Aqueous Two-Phase System. *Langmuir* **2014**, *30* (12), 3432–3440.
- 852 (29) Rodríguez-Cabello, J. C.; Girotti, A.; Ribeiro, A.; Arias, F. J.
853 Synthesis of genetically engineered protein polymers (recombinamers)
854 as an example of advanced self-assembled smart materials. *Methods*
855 *Mol. Biol. (N. Y., NY, U. S.)* **2012**, *811*, 17–38.
- 856 (30) Ritger, P. L.; Peppas, N. A. A simple equation for description of
857 solute release I. Fickian and non-fickian release from non-swelling
858 devices in the form of slabs, spheres, cylinders or discs. *J. Controlled*
859 *Release* **1987**, *5* (1), 23–36.
- 860 (31) Wilhelmus, K. R. The Draize eye test. *Surv. Ophthalmol.* **2001**,
861 *45* (6), 493–515.
- 862 (32) Chambers, W. A.; Green, S.; Gupta, K. C.; Hill, R. N.; Huntley,
863 K.; Hurley, P. M.; Lambert, L. A.; Lee, C. C.; Lee, J. K.; Liu, P. T.; et al.
864 Scoring for eye irritation tests. *Food Chem. Toxicol.* **1993**, *31* (2), 111–
865 5.
- 866 (33) Mehta, S. B.; Lewus, R.; Bee, J. S.; Randolph, T. W.; Carpenter,
867 J. F. Gelation of a monoclonal antibody at the silicone oil-water
868 interface and subsequent rupture of the interfacial gel results in
869 aggregation and particle formation. *J. Pharm. Sci.* **2015**, *104* (4), 1282–
870 90.
- 871 (34) Tung, C.-Y. M.; Dynes, P. J. Relationship between viscoelastic
872 properties and gelation in thermosetting systems. *J. Appl. Polym. Sci.*
873 **1982**, *27* (2), 569–574.
- 874 (35) Reguera, J.; Urry, D. W.; Parker, T. M.; McPherson, D. T.;
875 Rodríguez-Cabello, J. C. Effect of NaCl on the Exothermic and
876 Endothermic Components of the Inverse Temperature Transition of a
877 Model Elastin-like Polymer. *Biomacromolecules* **2007**, *8* (2), 354–358.
- 878 (36) Nowak, A. P.; Breedveld, V.; Pakstis, L.; Ozbas, B.; Pine, D. J.;
879 Pochan, D.; Deming, T. J. Rapidly recovering hydrogel scaffolds from
880 self-assembling diblock copolypeptide amphiphiles. *Nature* **2002**, *417*
881 (6887), 424–8.
- 882 (37) Mehta, S. B.; Carpenter, J. F.; Randolph, T. W. Colloidal
883 Instability Fosters Agglomeration of Subvisible Particles Created by
884 Rupture of Gels of a Monoclonal Antibody Formed at Silicone Oil-
885 Water Interfaces. *J. Pharm. Sci.* **2016**, *105* (8), 2338–48.
- 886 (38) Sosnik, A.; das Neves, J.; Sarmento, B. Mucoadhesive polymers
887 in the design of nano-drug delivery systems for administration by non-
888 parenteral routes: A review. *Prog. Polym. Sci.* **2014**, *39* (12), 2030–
889 2075.
- 890 (39) Greaves, J. L.; Wilson, C. G. Treatment of diseases of the eye
891 with mucoadhesive delivery systems. *Adv. Drug Delivery Rev.* **1993**, *11*
892 (3), 349–383.
- 893 (40) Murube, J.; Paterson, A.; Murube, E., Classification of Artificial
894 Tears. In *Lacrimal Gland, Tear Film, and Dry Eye Syndromes 2*;
895 Sullivan, D., Dartt, D., Meneray, M., Eds.; Springer US, 1998; Vol. 438,
896 pp 693–704.
- 897 (41) Tiffany, J. M. Tears in health and disease. *Eye* **2003**, *17* (8),
898 923–926.
- 899 (42) Andres-Guerrero, V.; Vicario-de-la-Torre, M.; Molina-Martinez,
900 I. T.; Benitez-del-Castillo, J. M.; Garcia-Feijoo, J.; Herrero-Vanrell, R.
Comparison of the in vitro tolerance and in vivo efficacy of traditional
timolol maleate eye drops versus new formulations with bioadhesive
polymers. *Invest. Ophthalmol. Visual Sci.* **2011**, *52* (6), 3548–56.
(43) Noecker, R.; Miller, K. V. Benzalkonium chloride in glaucoma
medications. *Ocul. Surf.* **2011**, *9* (3), 159–62.
(44) Pisella, P. J.; Pouliquen, P.; Baudouin, C. Prevalence of ocular
symptoms and signs with preserved and preservative free glaucoma
medication. *Br. J. Ophthalmol.* **2002**, *86* (4), 418–423.
(45) Jaenen, N.; Baudouin, C.; Pouliquen, P.; Manni, G.; Figueiredo,
A.; Zeyen, T. Ocular symptoms and signs with preserved and
preservative-free glaucoma medications. *Eur. J. Ophthalmol.* **2007**, *17*
(3), 341–349.
(46) Ishibashi, T.; Yokoi, N.; Kinoshita, S. Comparison of the short-
term effects on the human corneal surface of topical timolol maleate
with and without benzalkonium chloride. *J. Glaucoma* **2003**, *12* (6),
486–90.
(47) Gonzalez, A.; Tartara, L. I.; Palma, S. D.; Alvarez Igarzabal, C. I.
Crosslinked soy protein films and their application as ophthalmic drug
delivery system. *Mater. Sci. Eng., C* **2015**, *51*, 73–9.
(48) Calles, J. A.; Tartara, L. I.; Lopez-Garcia, A.; Diebold, Y.; Palma,
S. D.; Valles, E. M. Novel bioadhesive hyaluronan-itaconic acid
crosslinked films for ocular therapy. *Int. J. Pharm.* **2013**, *455* (1–2),
48–56.
(49) Rincon, A. C.; Molina-Martinez, I. T.; de Las Heras, B.; Alonso,
M.; Bailez, C.; Rodriguez-Cabello, J. C.; Herrero-Vanrell, R.
Biocompatibility of elastin-like polymer poly(VPAVG) microparticles:
in vitro and in vivo studies. *J. Biomed. Mater. Res., Part A* **2006**, *78A*
(2), 343–351.